Journal of Catalysis **199,** 41–47 (2001)
doi:10.1006/jcat.2000.3156, available online at http://www.idealibrary.com on IDEAL®

Effect of NH_4^+ Exchange on Hydrophobicity and Catalytic Properties of Al-Free Ti–Si–beta Zeolite

Masaru Ogura,* Shin-ichi Nakata,† Eiichi Kikuchi,* and Masahiko Matsukata*,[1]

*Department of Applied Chemistry, Waseda University, Okubo, Shinjuku, Tokyo 169-8555, Japan; and †Department of Materials-Process Engineering & Applied Chemistry for Environments, Faculty of Engineering and Resources Science, Akita University, Tegata Gakuen-cho, Akita 010-8502, Japan

Received June 26, 2000; accepted December 18, 2000; published online March 7, 2001

Al-free Ti–Si–beta was synthesized by a steam-assisted crystallization (SAC) method using tetraethylammonium hydroxide as a structure-directing agent. It was noted that Na in a parent gel was essential for synthesizing highly crystalline Ti–Si–beta by means of the SAC method. An absorption band at 225 nm, assigned to isolated Ti species, and another band at around 270 nm appeared in the UV spectra of the Ti–Si–beta. The latter absorption band decreased upon ion exchange of as-synthesized materials with 1 M aqueous NH_4NO_3 solution, and this treatment did not change the SiO_2/TiO_2 molar ratio in Ti–Si–beta. The Q^3 signal in the ^{29}Si-NMR spectrum almost disappeared and the amount of H_2O adsorbed decreased due to the NH_4^+ exchange of Ti–Si–beta. The NH_4^+ exchange resulted in a higher catalytic activity of the zeolite for cyclohexene epoxidation with H_2O_2 and a high selectivity toward epoxide compared with the H_2SO_4-treated Ti–Si–beta and Al-containing Ti–beta samples prepared in this study. Summarizing these results, the NH_4^+ exchange of Ti–Si–beta zeolite is found to induce a hydrophobic environment around Ti sites without detitanation from the zeolite framework. © 2001 Academic Press

Key Words: **Ti–beta; steam-assisted crystallization; NH_4^+ exchange; hydrophobicity.**

INTRODUCTION

Microporous materials containing hetero-atoms, which are incorporated into the materials' framework, are of great interest for selective catalytic reactions, and much attention has been focused on reactions using Ti-containing metallosilicates (1). Since TS-1, which involves Ti in MFI topology, has been reported to show outstanding properties with regard to epoxidation reactions (2–4), much research has been performed on Ti-containing zeolites, including not only TS-1 but also Ti–ZSM-12 (5), TS-2 (6), and Ti–ZSM-48 (7). Incorporation of Ti into zeolite structures imparts oxidation activity for synthesis of various organic intermediates. In particular, liquid phase epoxidation of olefins with H_2O_2 was found to proceed more preferably on Ti sites incorporated into the zeolite framework than on those in amorphous TiO_2–SiO_2. However, most of the studies on catalysis have been performed using TS-1, which has a 10-membered ring pore opening. The pore diameter of the zeolite limits its application in smaller hydrocarbon molecules. Several studies have recently appeared on the synthesis and catalytic activity of Ti–beta zeolite (8–11) in order to overcome such a limitation.

We have reported a new crystallization method, a dry gel conversion (DGC) technique, and have demonstrated the crystallization of zeolite beta from a dry gel containing tetraethylammonium hydroxide (TEAOH) as a structure-directing agent (SDA) (12–14). Quaternary amines such as tetrapropylammonium hydroxide (TPAOH) are often used as SDAs for synthesis of MFI and are not volatile. When being used, such a nonvolatile SDA can be involved in a dry gel. Only steam is supplied from the gas phase in crystallizing the SDA-containing dry gel, the method of which is called "steam-assisted crystallization (SAC)" (15). By using the SAC method, beta, which is difficult to crystallize using conventional hydrothermal synthetic methods (16–18), can be obtained with a wide range of SiO_2/Al_2O_3 molar ratios from 30 to infinity, whereas dibenzyldimethyl ammonium cation (19) or TEAOH–hydrogen fluoride (HF) mixture (20) is required as SDAs for the hydrothermal crystallization of pure silica–beta, Si–beta. Al-free Ti–beta was also synthesized by TEAOH along with HF using the hydrothermal synthetic method (21), leading to the creation of Ti sites surrounded by a hydrophobic environment (22). On the other hand, the SAC method enables us to crystallize Si–beta without fluorine.

Tatsumi *et al.* (23–25) have recently reported the crystallization of highly active Al-containing Ti–beta. They reported that the epoxidation reactions of cyclic, linear, and branched alkenes using H_2O_2 selectively occur on Ti–Al–beta obtained by the SAC method. These reactions proceed on Ti sites surrounded by a hydrophobic environment, which can be accomplished in zeolites obtained by the SAC method compared with those prepared hydrothermally.

---

[1] To whom correspondence should be addressed. Fax: +81-3-5286-3850. E-mail: mmatsu@mn.waseda.ac.jp.

In this study, aluminum-free Ti-containing beta zeolite is synthesized by means of the SAC method using TEAOH to give a hydrophobic environment to Ti species relatively higher than that given to those on Ti–Al–beta. Further, we show a simple way to further improve the hydrophobic environment surrounding the Ti species in Ti-containing beta zeolites.

EXPERIMENTAL

Al-free Ti–Si–beta was prepared from dry gels having compositions of $SiO_2 : 0.0033–0.1\ TiO_2 : 0.44$ TEAOH : 0–0.096 Na_2O. These gels were prepared by mixing silica (fumed, Aldrich), NaOH (4 M aqueous solution, Wako Pure Chemical), and TEAOH (20% in water, Merck). An aqueous solution containing required amounts of $Ti(OC_4H_9)_4$ (monomer, Kanto Chemical) and H_2O_2 (31% in water, MGC) was added after stirring for 1 h at 293 K. The amount of H_2O_2 was determined to have a H_2O_2/TiO_2 molar ratio of 20. Typically, 1.5 g of silica, 1.2 ml of NaOHaq, 6.7 g of TEAOHaq, 0.17 g of $Ti(OBu)_4$, and 1 ml of H_2O_2 were used for one-batch synthesis with $SiO_2/TiO_2 = 50$. The mixture was heated to 353 K after stirring for 2 h at 293 K and dried while stirring. A dried gel, ca. 3 g, was crushed into powder and placed in a Teflon cup inside an autoclave. Water, ca. 0.5 ml, was poured as a source of steam onto the bottom of the autoclave. Crystallization of the dry gel was carried out at 413 K for 8 days. Since the volume of the autoclave was 100 cm^3 and the saturated water vapor pressure at 413 K was ca. 5 atm, the amount of H_2O in the autoclave was sufficiently high to achieve the water vapor pressure necessary for saturation during crystallization.

Before the measurements of the UV spectra, H_2O adsorption, and catalytic activities, all samples were calcined in an electric furnace. The heating rate was controlled at 1.5 K/min. The sample was heated to 808 K and kept at this temperature for 12 h. The as-synthesized sample after calcination was named Na^+/Ti–Si–beta.

H_2SO_4 washing treatment (26) was conducted to eliminate Ti species in an amorphous phase. As-synthesized Ti–Si–beta was dispersed in a 0.5 M aqueous solution of H_2SO_4 at room temperature and stirred for 2 h, followed by filtration and washing with distilled water to obtain H_2SO_4/Ti–Si–beta. Separately, treatment of as-synthesized Ti–Si–beta with a 1 M aqueous NH_4NO_3 solution at 353 K for 2 h was conducted five times for ion exchange into the NH_4^+-type samples (NH_4NO_3/Ti–Si–beta).

For comparison, Ti–Al–beta samples with SiO_2/Al_2O_3 molar ratios of 380 and 730 and with a SiO_2/TiO_2 molar ratio of 50 were prepared according to the literature (23) and were designated Ti–Al–beta380 and Ti–Al–beta730, respectively. $Al_2(SO_4)_3$ was used as an Al source. These samples after calcination at 808 K were ion exchanged with a 1 M NH_4NO_3 aq, followed by calcination at 773 K to form H^+/Ti–Al–beta.

Zeolite samples were dissolved in a hydrofluoric acid solution and the chemical compositions were determined by means of inductively coupled plasma atomic emission spectroscopy (ICP-AES). X-ray diffraction patterns were measured using a RINT 2000 (Rigaku Instrument Corp.) with Cu$K\alpha$ radiation for confirming the structure and crystallinity of the products. The morphology and particle size of the products were evaluated by means of field-emission scanning electron microscopy (FE-SEM, S4500, Hitachi Corp.). Diffuse reflectance ultraviolet absorption spectra were recorded with a UV3101 (JEOL Corp.) for identifying the Ti coordination state in the products. H_2O adsorption studies on the samples at 298 K were conducted using a Belsorp 18 (BEL Japan, Inc.). ^{29}Si-MAS NMR spectroscopic study was performed using a GSX-400, JEOL, at a ^{29}Si frequency of 79.3 MHz, a spinning rate of 5 kHz with a 45° pulse length of 4.2 μs, and a recycle time of 60 s. The ^{29}Si chemical shifts were reported relative to tetramethylsilane.

Catalytic activities of the Ti-containing samples were evaluated in terms of cyclohexene oxidation reaction with H_2O_2. A solution of 30 mmol of cyclohexene and 10 mmol of H_2O_2 in 300 ml of acetonitrile solvent was used. A zeolite sample weighing 50 mg was added into the solution and the solution was heated moderately to 323 K while stirring in a water bath. Reaction was performed at that temperature for 2 h. After the reaction, the solution was filtered and analyzed by GC-FID to determine cyclohexene conversion and selectivity for epoxide and the other products.

RESULTS AND DISCUSSION

Crystallization of Ti-Containing Zeolites by SAC Method and Their Physicochemical Properties

Table 1 lists the synthetic conditions and the products obtained by the SAC method. Ti–Si–beta was not obtained without adding Na^+ to the dry gel which agrees closely with a previous suggestion (23, 24) that Na^+ is indispensable for the crystallization of dry gel into the Ti–Al–beta phase. As

TABLE 1

Crystallization Results of Ti–Si–Beta

Temperature (K)				
Gel aging	Gel drying	Crystallization	Na_2O/SiO_2	Product
293	353	413	0	Amor.
			0.042	BEA + Amor.
			0.096	BEA
			0.160	BEA + quartz
293	353	453	0.096	Amor. + MFI
277	353	413	0.096	Amor.
—	353	413	0.096	Amor.
293	333	413	0.096	BEA + amor.

Note. Gel composition, $SiO_2 : 0.02\ TiO_2 : 0.44$ TEAOH : $n Na_2O$.

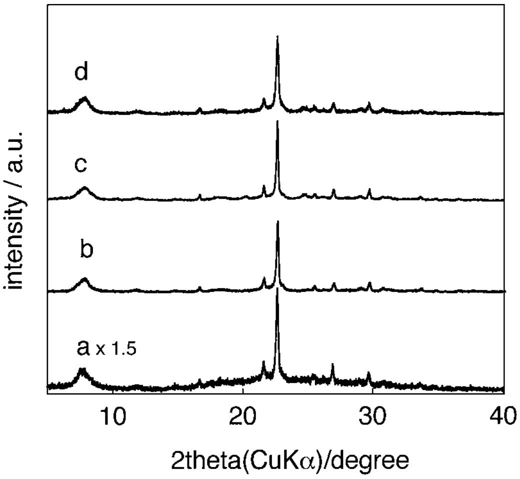

FIG. 1. XRD patterns for as-synthesized products. (a) Si–beta, (b) Al–beta380, (c) Ti–Si–beta (SiO_2/TiO_3 ratio = 50.), (d) Ti–Al–beta380 (SiO_2/TiO_2 ratio = 50.).

revealed in Table 1, the amount of Na^+ was very important for crystallization. The most adequate ratio of Na_2O/SiO_2 was 0.096. Below 0.096 of the Na_2O/SiO_2 ratio, an amorphous phase was formed, while a dense phase appeared along with the beta with increasing amounts of Na^+.

Tatsumi *et al.* (23, 24) have reported that the best temperature for crystallization of Ti–Al–beta was 403 K for 96 h, and subsequently at 448 K for 18 h. In the case of Ti–Si–beta, the adequate temperature for crystallization was 413 K, and the diffraction peaks assigned to the BEA structure started to appear in the XRD pattern after 6 days of crystallization. Highly crystallized Ti–Si–beta was obtained after 8 days. The MFI phase was formed along with BEA at above 413 K.

When using the SAC method, the aging conditions of a hydrogel were found to be critical in governing the crystallinity of products. Among the conditions tested in this study, aging a hydrogel at 293 K for 2 h while vigorously stirring is needed to synthesize Ti–Si–beta. The temperature necessary to achieve a high Ti–Si–beta crystallinity during the drying of the gel was higher than 353 K.

Figure 1 shows the X-ray diffraction patterns of as-synthesized products. The XRD patterns show a sharp reflection peak at around 22.5° attributed to BEA structure with high intensities, showing that each sample was obtained at a high level of crystallinity. Judging from the diffraction pattern with the hump, Si–beta (Fig. 1a) appeared to have a lower level of crystallinity than did other beta zeolites containing Al (Fig. 1b) and/or Ti (Figs. 1c and d).

Zeolites with fairly uniform particle sizes were typically observed in the SEM views, as shown in Fig. 2. Si–beta (Fig. 2a) and Ti-containing Si–beta (Fig. 2b) exhibited larger particle sizes, ca. 700 nm for Si–beta and ca. 500 nm for Ti–Si–beta. Their sizes became much smaller by adding a small amount of Al: the particle size of Ti–Al–beta380 (Fig. 2c) was about 100 nm. Perez-Pariente *et al.* have claimed in studies of zeolite beta crystallization by the hydrothermal

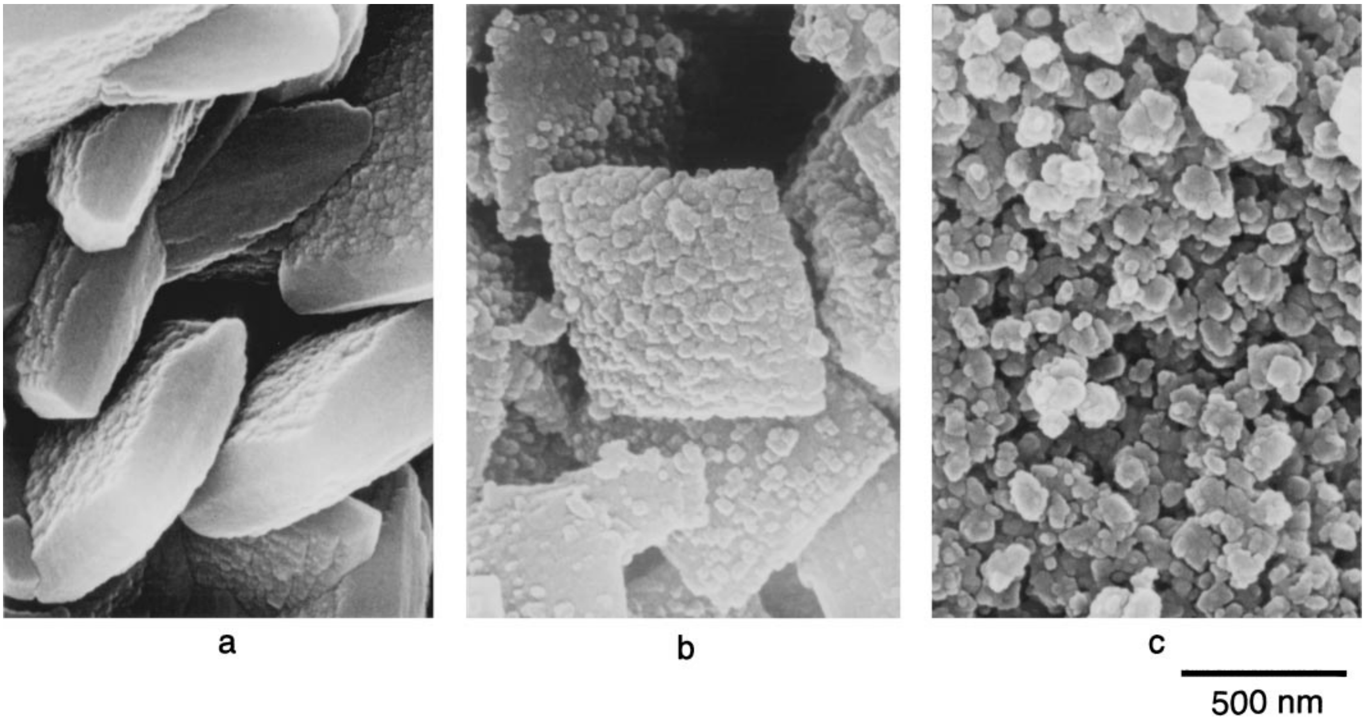

FIG. 2. SEM images for Si–beta (a), Ti–Si–beta (b), and Ti–Al–beta380 (c).

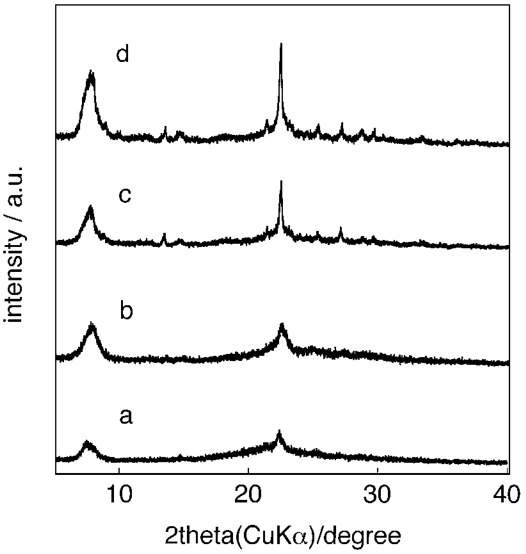

FIG. 3. XRD patterns for Si–beta (a), Na^+/Ti–Si–beta (b), H_2SO_4/Ti–Si–beta (c), and NH_4NO_3/Ti–Si–beta (d) after calcination at 808 K for 12 h.

synthetic method that Al plays a role in the rapid nucleation of the hydrogel to beta (16). There might be a small amount of nuclei in the dry gels for Si–beta or Ti–Si–beta, resulting in the formation of larger particles in the absence of Al.

Effect of NH_4^+ Exchange of Ti–Si–Beta

In the previous work, we found that ion exchange of Al–beta with NH_4NO_3 aqueous solution is effective in improving stability against calcination even at 1373 K (13). This effect might be due to the removal of Na^+ remaining in the zeolite without the collapse of the zeolite framework. Figure 3 shows the XRD patterns of Si–beta and Ti–Si–beta samples after calcination at 808 K for 12 h. After the calcination, the diffraction peaks of Si–beta (Fig. 3a) had almost disappeared, indicating that Si–beta exhibits low stability against calcination. Similar instability can be observed for Na^+/Ti–Si–beta, as shown in Fig. 3b. On the other hand, the intensities of the diffraction peaks from H_2SO_4-treated Ti–Si–beta (Fig. 3c) decreased slightly. Moreover, NH_4^+-exchanged Ti–Si–beta (Fig. 3d) was hardly collapsed by calcination at 808 K: the intensity of the diffraction peak from the sample remained unchanged.

These Ti-containing zeolite samples underwent a catalytic activity test, cyclohexene epoxidation with H_2O_2. Table 2 shows the effect of treatment on the catalytic performance of Ti–Si–beta for epoxidation using acetonitrile as a solvent. Ti–Si–beta samples showed higher conversions than did H^+/Ti–Al–beta, while they showed lower selectivity toward epoxide. Other products were cyclohexene-1-ol and a small amount of peroxide such as cyclohexyl hydroperoxide. H_2SO_4 washing was found to obviously improve the catalytic performance of Na/Ti–Si–beta: the selectivity toward epoxide increased from 45 to 62%. A much higher level of conversion was obtained using NH_4NO_3/Ti–Si–beta. The epoxide selectivity became very close to those of H^+/Ti–Al–beta380 and H^+/Ti–Al–beta730. If all the Ti in NH_4NO_3/Ti–Si–beta was located in the framework position, the turnover number was predicted to be 648 mol/mol Ti. The values reported in the literature were 9.2/h at 298 K (27), 289 at 343 K (28), and 677 at 333 K (23). Compared with these results, the catalytic activity of NH_4NO_3/Ti–Si–beta in our work was comparable or slightly higher.

TABLE 2

Epoxidation of Cyclohexene with H_2O_2 on Ti–Beta

Sample	Cyclohexene conversion (%)	Epoxide selectivity (%)
Si–beta	0	0
Na^+/Ti–Si–beta	19	45
H_2SO_4/Ti–Si–beta	28	62
NH_4NO_3/Ti–Si–beta	35	89
H^+/Ti–Al–beta730	11	98
H^+/Ti–Al–beta380	11	98

Note. Reaction conditions: cyclohexene, 30 mmol; H_2O_2, 10 mmol; CH_3CN as a solvent. Catalyst, 50 mg; reaction temperature, 323 K; duration, 2 h.

Figure 4 shows the UV spectra for as-synthesized Na^+/Ti–Si–beta, H_2SO_4/Ti–Si–beta, and NH_4NO_3/Ti-Si-beta. The

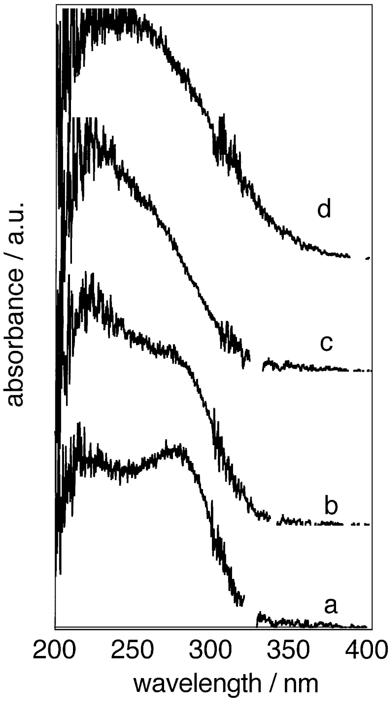

FIG. 4. Ultraviolet absorption spectra for Ti–Si–beta with various pretreatments. (a) As-synthesized Ti–Si–beta, (b) Na^+/Ti–Si–beta, (c) H_2SO_4/Ti–Si–beta, (d) NH_4NO_3/Ti–Si–beta. SiO_2/TiO_2 ratio = 50.

UV spectra have an intense but broad band between 205 and 250 nm. A band at 225 nm has been assigned to isolated titanium in framework tetrahedral coordination (29). The existence of the band suggests the presence of Ti at a framework position in zeolite. In addition, an absorption band appeared at around 270 nm on as-synthesized Ti–Si–beta (Fig. 4a) and Na^+/Ti–Si–beta (Fig. 4b). It has been previously reported that the band at 270 nm comes from extraframework titanium (30) partially polymerized hexacoordinated Ti species (31). The band at 270 nm is clearly observed in as-synthesized Ti–Si–beta (Fig. 4a), and the intensity of the band was slightly decreased by calcination (Fig. 4b). This indicates that the number of Ti–OH sites where H_2O is adsorbed decreased upon calcination.

The UV spectrum of H_2SO_4-washed Ti–Si–beta is also shown in Fig. 4c, where the absorption band near 270 nm disappeared. As reported by Tatsumi *et al.* (23, 24), H_2SO_4 washing led to a change in SiO_2/TiO_2 ratio, implying that Ti might be eliminated from the framework by this treatment.

A decrease in the intensity of the UV band at 270 nm can also be seen on NH_4NO_3/Ti–Si–beta, as shown in Fig. 4d. The SiO_2/TiO_2 ratio in Ti–Si–beta did not change after the ion exchange with NH_4^+. The Ti atom was, thus, hardly eluted in aqueous NH_4NO_3 solution. This result indicates that most of Ti in as-synthesized Ti–Si–beta is incorporated into the zeolite framework. Although some defect sites such as Si–O–Na or Ti–O–H in Ti–Si–beta connected to H_2O molecules to form a six-coordination state, the ion exchange with NH_4^+, followed by calcination, transformed those sites not to adsorb H_2O. On the other hand, from the results of changing Si/Ti ratios produced by washing Ti–Si–beta with H_2SO_4, this treatment eliminates the Ti species from the zeolite where H_2O can be adsorbed.

Figure 5 shows the adsorption isotherms of H_2O on the calcined samples of various Ti–Si–beta and H^+/Ti–Al–beta. From the isotherms at the value of low P/P_0, the amount of H_2O adsorbed on Na/Ti–Si–beta was comparable with that on H^+/Ti–Al–beta380. The amounts of H_2O adsorbed on each zeolite in the low range of P/P_0 calculated according to the Langmuir equation are summarized in Table 3. These results indicate that Na^+/Ti–Si–beta has adsorption sites for H_2O as much as H^+/Ti–Al–beta380. It might be reasonable that the amount of H_2O adsorbed on H^+/Ti–Al–beta730 was smaller than that adsorbed on H^+/Ti–Al–beta380. However, the amounts of adsorbed H_2O did not correlate with the amount of Al. There exists another type of adsorption site for H_2O such as defect sites, Si–O–Na. Interestingly, the amount of adsorbed H_2O on Ti–Si–beta was decreased by H_2SO_4 washing revealing that the sites, which can adsorb the H_2O molecule, remaining on Ti–Si–beta can be removed by H_2SO_4 washing. An initial isotherm slope was much smaller on NH_4NO_3/Ti–Si–beta and the total amount of adsorbed H_2O was less than that on any other sample tested.

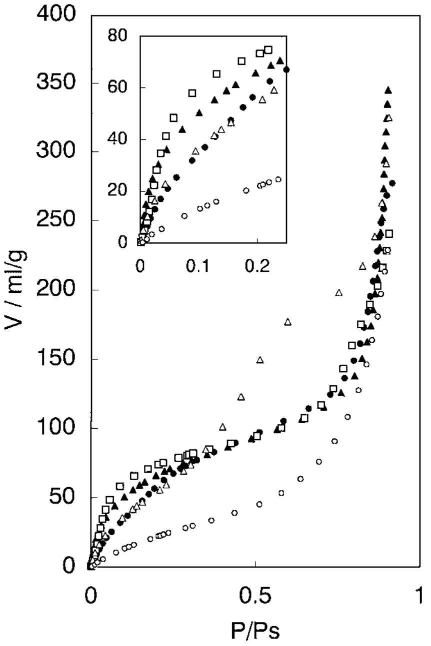

FIG. 5. Adsorption isotherms of H_2O on Ti–beta samples. (□) Na^+/Ti–Si–beta, (△) H_2SO_4/Ti–Si–beta, (○) NH_4NO_3/Ti–Si–beta, (▲) H^+/Ti–Al–beta730, (●) H^+/Ti–Al–beta380. SiO_2/TiO_2 ratio = 50.

It can be considered that H_2O molecules are adsorbed on defect sites, even in a pure silica zeolite structure, such as the Si–OH groups. Figure 6 shows the ^{29}Si MAS-NMR spectra for zeolite samples. As shown in Fig. 6a, Si–beta has a larger amount of Q^3 that appears at the chemical shift of −100 ppm, suggesting that the crystallinity is low because an amorphous phase remains or many defect sites exist. The products containing Ti seem to have smaller amounts of Q^3 than does the pure silica phase. On Na^+/Ti–Si–beta, the amount of Q^3 signal was much less than that on Si–beta. The intensity of the Q^3 signal was decreased by H_2SO_4 washing. A further decrease can be observed in the sample ion-exchanged with NH_4^+. It is noteworthy that the effect

TABLE 3

Amounts of H_2O Adsorbed on Ti–Beta Samples[a]

Sample	V_{H_2O} (ml g^{-1})
Na^+/Ti–Si–Beta	62.7
H_2SO_4/Ti–Si–Beta	16.4
NH_4NO_3/Ti–Si–Beta	10.9
H^+/Ti–Al–Beta380	57.3
H^+/Ti–Al–Beta730	49.1

[a] The values are calculated from the isotherms of Fig. 5 according to Langmuir equation in the low range of P/P_0 from 0.05 to 0.30.

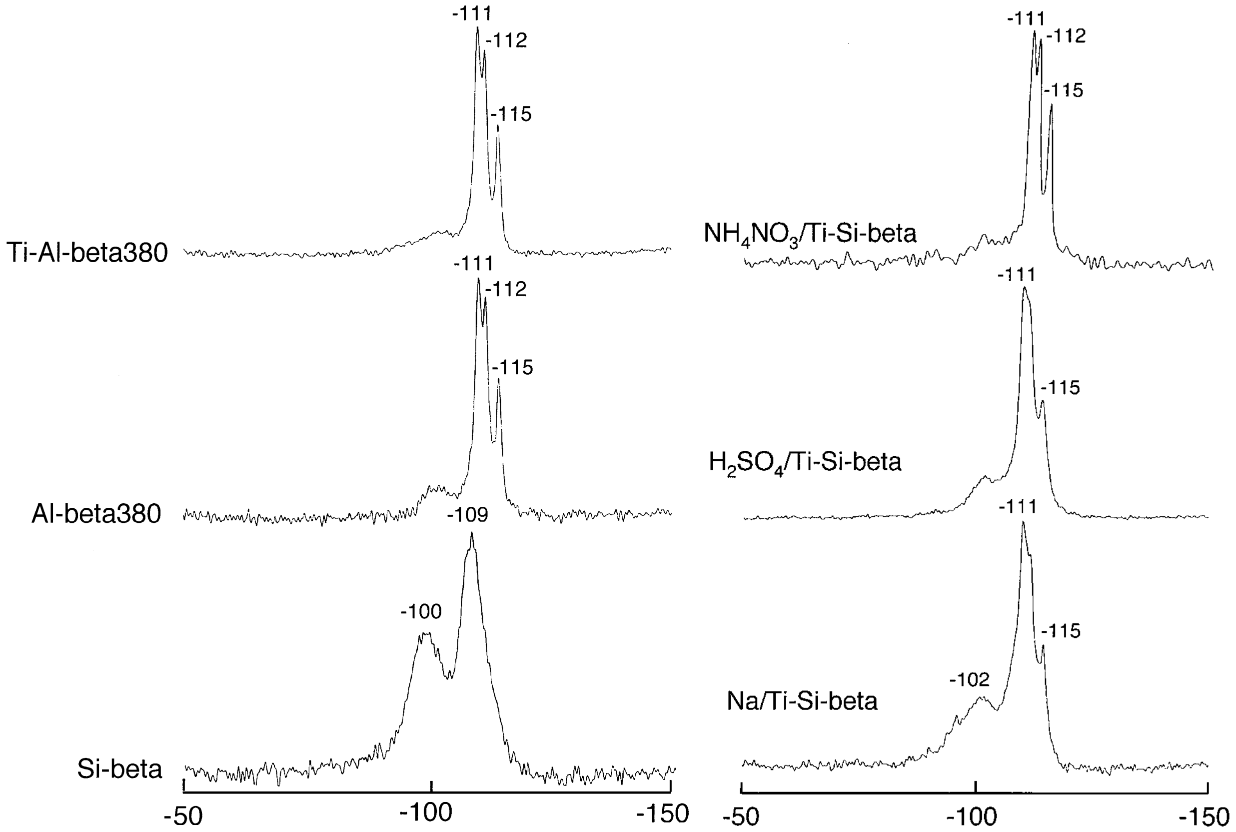

FIG. 6. ^{29}Si MAS-NMR spectra for Si–beta, Na^+/Ti–Si–beta, H_2SO_4/Ti–Si–beta, and NH_4NO_3/Ti–Si–beta. SiO_2/TiO_2 ratio of Ti-containing samples was 50.

of NH_4^+ exchange can be seen on the narrower width of the Q^4 signal in the spectrum, indicating that the crystallinity of Ti–Si–beta is enhanced. It has been reported that incorporation of Ti inside the framework of beta caused a broadening of Q^4 signals and that three bands at ca. −112, −113, and −116 ppm could be observed on Ti–Si–beta below 1.05 Ti per unit cell (22). In the present work, however, these three bands clearly appeared on NH_4NO_3/Ti–Si–beta at 1.28 Ti per unit cell. These results from the H_2O adsorption isotherm and ^{29}Si-NMR suggest that the synthesis of aluminum-free Ti–Si–beta and its treatment with NH_4NO_3 enable us to achieve Ti sites in a hydrophobic environment without detitanation from the zeolite framework.

The effect of NH_4NO_3 treatment for Ti–Si–beta is suggested and illustrated in Fig. 7. From the chemical analyses of N atoms occluded in as-synthesized samples (results are not shown), fully crystallized Ti–Si–beta has ca. 6 TEA^+ cations per unit cell even if Ti content is changed from 0 to 2.1 Ti per unit cell; therefore, we consider that the TEA^+ cation is located on $SiO^{\delta-}$ sites. Na^+ should be located at a slightly negative-charged Si–$O^{\delta-}$ site, which gives a Q^3 signal in a ^{29}Si-NMR spectrum. Such Na^+ remains after calcination, creating H_2O adsorption sites such as Si–$O^{\delta-}$ and next-neighboring Ti–OH. It was confirmed by chemical analysis that Na^+ hardly remained on the Ti–Si–beta sample after the NH_4NO_3 treatment. Heat treatment causes the NH_4^+ cation to release a NH_3 molecule along with the

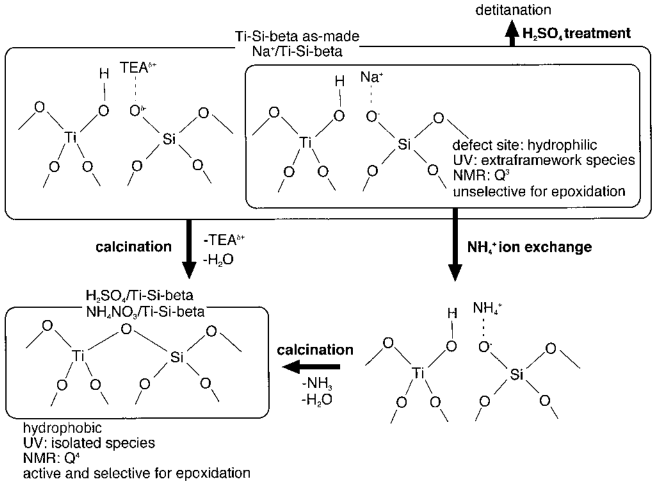

FIG. 7. Effect of NH_4^+ exchange on hydrophobicity of Ti–Si–beta zeolite.

formation of Si–OH groups that are possibly dehydrated and condensed with a next-nearest neighboring Si–O–H or Ti–O–H to create a Si–O–Si or a Si–O–Ti bond. The hydrophobic environment around Ti sites is established by eliminating hydroxyl groups and thus leads to a higher selectivity toward epoxide in epoxidation reaction with H_2O_2.

Based on the results of this work, we suggest that the NH_4NO_3 treatment effectively reduces the number of defect sites. We successfully obtained beta zeolite with fewer defect sites, resulting in high thermal stability (13). NH_4NO_3/beta was stable even after calcination at 1373 K.

CONCLUSIONS

Al-free pure silica Si–beta and Ti-containing Si–beta were synthesized using the SAC method employing TEAOH as a SDA. Sodium cation is essential for the crystallization of beta. Also, the aging conditions of hydrogel were critical for the synthesis of highly crystalline Ti–Si–beta.

NH_4^+ exchange before calcination was found to decrease an UV absorption band at 270 nm without any change in the SiO_2/TiO_2 ratio in the zeolite. The ion exchange with NH_4^+ was also effective for the reduction of the amount of adsorbed H_2O and of the Q^3 signal, which corresponds to defect sites in zeolite, resulting in high hydrothermal stability. Though it plays an essential role in the synthesis of Ti–Si–beta by SAC, Na^+ needs to be eliminated in order to improve hydrophobicity. NH_4^+ exchange is useful in removing Na^+ cations and in creating Ti sites surrounded by a hydrophobic environment in zeolite, leading to higher catalytic activity for cyclohexene epoxidation with H_2O_2 and higher selectivity toward epoxide.

REFERENCES

1. Notari, B., *Adv. Catal.* **41**, 253 (1996).
2. Perego, G., Bellusi, G., Corno, C., Taramasso, M., Buonomo, F., and Esposito, A., *Stud. Surf. Sci. Catal.* **28**, 129 (1986).
3. Notari, B., *Catal. Today* **18**, 163 (1993).
4. Clerici, M. G., and Ingallina, P., *J. Catal.* **140**, 71 (1993).
5. Tuel, A., *Zeolites* **15**, 236 (1995).
6. Reddy, J. S., Kumar, R., and Ratnasamy, P., *Appl. Catal.* **A58**, L1 (1990).
7. Serrano, D. P., Li, H. X., and Davis, M. E., *J. Chem. Soc. Chem. Commun.* 745 (1992).
8. Camblor, M. A., Corma, A., Martinez, A., and Perez-Pariente, J., *J. Chem. Soc. Chem. Commun.* 589 (1992).
9. Davis, R. J., Liu, Z., Tabora, J. E., and Wieland, W. S., *Catal. Lett.* **34**, 101 (1995).
10. Dartt, C. B., and Davis, M. E., *Appl. Catal.* **A143**, 53 (1996).
11. Jahn, S. L., Nascente, P. A. P., and Cardoso, D., *Zeolites* **19**, 416 (1997).
12. Rao, P. R. H. P., and Matsukata, M., *Chem. Commun.* 1441 (1996).
13. Rao, P. R. H. P., Ueyama, K., and Matsukata, M., *Appl. Catal.* **A166**, 97 (1998).
14. Rao, P. R. H. P., Leon y Leon, C. A., Ueyama, K., and Matsukata, M., *Microporous Mesoporous Mater.* **21**, 305 (1998).
15. Matsukata, M., Ogura, M., Osaki, T., Rao, P. R. H. P., Nomura, M., and Kikuchi, E., *Top. Catal.* **9**, 77 (1999).
16. Perez-Pariente, J., Martens, J. A., and Jacobs, P. A., *Zeolites* **8**, 46 (1988).
17. Bhat, R. N., and Kumar, R., *J. Chem. Tech. Biotechnol.* **48**, 453 (1990).
18. Camblor, M. A., and Perez-Pariente, J., *Zeolites* **11**, 202 (1991).
19. van der Waal, J. C., Rigutto, M. S., and van Bekkum, H., *J. Chem. Soc. Chem. Commun.* 1241 (1994).
20. Camblor, M. A., Corma, A., and Valencia, S., *Chem. Commun.* 2365 (1996).
21. Blasco, T., Camblor, M. A., Corma, A., Esteve, P., Martinez, A., Prieto, C., and Valencia, S., *Chem. Commun.* 1996, 2367.
22. Blasco, T., Camblor, M. A., Corma, A., Esteve, P., Guil, J. M., Martinez, A., Perdigon-Melon, J. A., and Valencia, S., *J. Phys. Chem.* **B102**, 75 (1998).
23. Tatsumi, T., Xia, Q., and Jappar, N., *Chem. Lett.* 1997, 677.
24. Tatsumi, T., and Jappar, N., *J. Phys. Chem.* **B102**, 7126 (1998).
25. Jappar, N., Xia, Q., and Tatsumi, T., *J. Catal.* **180**, 132 (1998).
26. Khouw, C. B., and Davis, M. E., *J. Catal.* **151**, 77 (1995).
27. Corma, A., Camblor, M. A., Esteve, P., Martinez, A., and Perez-Pariente, J., *J. Catal.* **145**, 151 (1994).
28. van der Waal, J. C., Rigutto, M. S., and van Bekkum, H., *Appl. Catal.* **A167**, 331 (1998).
29. Boccuti, M. R., Rao, K. M., Zecchina, A., Leofanti, G., and Petrini, G., *Stud. Surf. Sci. Catal.* **48**, 133 (1988).
30. Kim, Y. L., Riley, R. L., Huq, M. J., Salim, S., Le, A. E., and Mallouk, T. E., *Mater. Res. Soc. Symp. Proc.* **233**, 145 (1991).
31. Blasco, T., Camblor, M. A., Corma, A., and Perez-Pariente, J., *J. Am. Chem. Soc.* **115**, 1806 (1993).